THE JOURNAL OF PHYSICAL CHEMISTRY B

ARTICLE

pubs.acs.org/JPCB

Optimized Unlike-Pair Interactions for Water−Carbon Dioxide Mixtures Described by the SPC/E and EPM2 Models

Lukas Vlcek,* Ariel A. Chialvo, and David R. Cole†

Chemical Sciences Division Geochemistry & Interfacial Sciences Group, Oak Ridge National Laboratory, Oak Ridge, Tennessee 37831-6110, United States

Supporting Information

ABSTRACT:

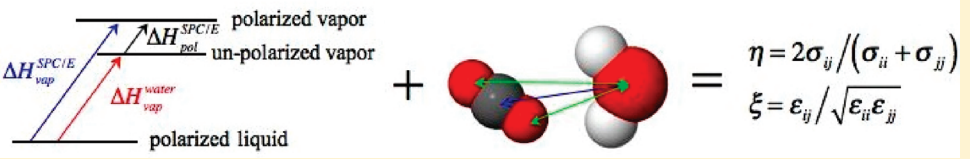

The unlike-pair interaction parameters for the SPC/E−EPM2 models have been optimized to reproduce the mutual solubility of water and carbon dioxide at the conditions of liquid−supercritical fluid phase equilibria. An efficient global optimization of the parameters is achieved through an implementation of the coupling parameter approach, adapted to phase equilibria calculations in the Gibbs ensemble, that explicitly corrects for the overpolarization of the SPC/E water molecule in the nonpolar CO_2 environments. The resulting H_2O-CO_2 force field accurately reproduces the available experimental solubilities at the two fluid phases in equilibria as well as the corresponding species tracer diffusion coefficients.

1. INTRODUCTION

Carbon dioxide−water systems are commonly found in the oil and gas industry, such as in enhanced oil recovery and natural gas streams, and frequently their presence in these environments are a matter of concern for the potential corrosion effects and pipe plugging due to hydrate formation. Renewed interest in the thermophysical behavior of carbon dioxide−water systems has been generated by numerous proposed processes including the CO_2-enhanced geothermal systems as sources of geothermal energy[1,2] and the CO_2 capture from power stations and subsequent storage in deep geologic formations as a means to mitigate global warming.[3] From a process design standpoint, carbon capture and sequestration requires an accurate description of carbon dioxide interactions with aqueous environments in contact with minerals at moderate temperatures and pressures.[4] From a microscopic perspective, we need accurate molecular models to gain understanding of the underlying physicochemical mechanisms at such environmental conditions.

A large number of H_2O[5] and CO_2[6−9] models have been developed with various degrees of complexity, but probably the most popular ones are the SPC/E[10] for liquid water and the EPM2[11] for near-critical carbon dioxide (see Table 1). The large body of published data, including force fields for the interaction of water and carbon dioxide with dissolved ions and mineral surfaces, provide a solid basis for the study of the H_2O-CO_2 mixtures at a variety of state conditions and compositions. A prerequisite for such a study is the appropriate description of the unlike-pair interactions between the two species, which are typically described in terms of combining rules. As far as we are aware, there has been no attempt to describe the binary mixture by the SPC/E and EPM2 models beyond the simple (conventional) combining rules, such as the Lorentz−Berthelot (LB) prescription.

The need for an adequate description of the unlike-pair interactions between different molecular species in a fluid mixture comes from the fact that those interactions are the actual sources of thermodynamic nonideality, measured by the deviation of an extensive mixture property $M(T,P,x)$ from the corresponding ideal solution $M^{E}(T,P,x) = M(T,P,x) - M^{IS}(T,P,x)$ at the same state conditions and composition.[12] For example, by invoking the definitions of an ideal solution by Lewis−Randall rule and the corresponding residual property $M^{res}(T,P,x) \equiv M(T,P,x) - M^{IG}(T,P,x)$, the thermodynamic excess property $M^{E}(T,P,x)$ becomes

$$M^{E}(T,P,x) = \sum_i x_i[M^{res}(T,P,x) - M_i^{O,res}(T,P)] \qquad (1)$$

where the superscripts E, res, IG, and O stand for excess, residual, ideal gas, and pure component properties, respectively. Considering that by definition the residual quantities measure the contributions of the intermolecular interactions to the system properties (i.e., zero interactions between ideal gas species), eq 1 indicates that excess properties involve contributions from differences of intermolecular interactions between species in solution, i.e., from their intermolecular interaction asymmetry. Consequently, excess (rather than mixing) quantities are the

Received: April 7, 2011
Revised: May 27, 2011
Published: June 06, 2011

Table 1. Parameters of the SPC/E[10] and EPM2[11] Models

atom type	σ_{ii} [Å]	ε_{ii} [kcal/mol]	q_i
O_W	3.166	0.65	−0.8476
H_W	0.0	0.0	0.4238
C_C	2.757	0.2339	0.6512
O_C	3.033	0.6694	−0.3256

most sensitive properties for the analysis of the impact of the unlike-pair interactions on the mixture properties by molecular-based theory and simulation.[13−17]

Since the pioneering work of Hudson, Kohler, and colleagues on the quantum mechanical-based combining rules for the unlike-pair interactions of spherical[18−20] and nonspherical[21] molecules, numerous alternative algebraic forms for these rules have been proposed based on a variety of empirical and theoretical approaches.[22−30] Regardless of their dependence with the corresponding like-pair interactions (i.e., pure component), the proposed combining rules for the energy− and size-parameters can be expressed as "deviations" (see eq 2 below) from a common reference, i.e., the LB rules, even when the actual combining rules are not completely independent from each other (e.g., see Kong's rules[26]).

The first simulation study of the effect of unlike-pair interaction parameters on the excess properties of model fluids was done by Singer and Singer[31] who introduced the parameters η and ξ to account for the deviations of the actual unlike-pair interactions from the corresponding LB combining rules for the Lennard-Jones (LJ) size and energy parameters, respectively, i.e.,

$$\eta = \frac{2\sigma_{ij}}{(\sigma_{ii}+\sigma_{jj})}; \quad \xi = \frac{\varepsilon_{ij}}{\sqrt{\varepsilon_{ii}\varepsilon_{jj}}} \tag{2}$$

The appeal of eq 2 is the direct identification of η and ξ as "coupling parameters" in Kirkwood's versatile approach to the determination of free energies[32,33] and its adaptation to the assessment of the effect of the strength of the unlike-pair interactions on the thermodynamic excess properties of mixtures.[14,16] This effort was the first of its kind to demonstrate that small deviations from the Lorentz rule exhibits a stronger effect on the resulting excess thermodynamic properties in simple fluid mixtures than deviations from the Berthelot rule counterpart. The subject has been recently revisited by several groups[34−40] by targeting diverse aspects of the combining rules and the resulting microstructural as well as thermophysical mixture behavior.

Not surprisingly, the unlike-pair interaction parameters have been most commonly used simply as adjustable parameters in an effort to get better agreement between model predictions and experimental data.[17,41−47] Obviously this adjustment becomes a sound approach provided that the models for the pure components already accurately describe the microstructural and thermodynamic behavior of these fluids at the state conditions of interest, i.e., when the adjustment would not absorb the inaccuracies of the pure component model properties. This is precisely the case for the EPM2[11] and the SPC/E[10] models in the description of the behavior of pure carbon dioxide and water, respectively. These two popular and well-characterized models use rigid geometries and involve LJ plus (fixed) partial charges for the model electrostatics (for details, see the original publications[10,11]) to describe the polar and quadrupolar nature of water and carbon dioxide, respectively. The resulting models

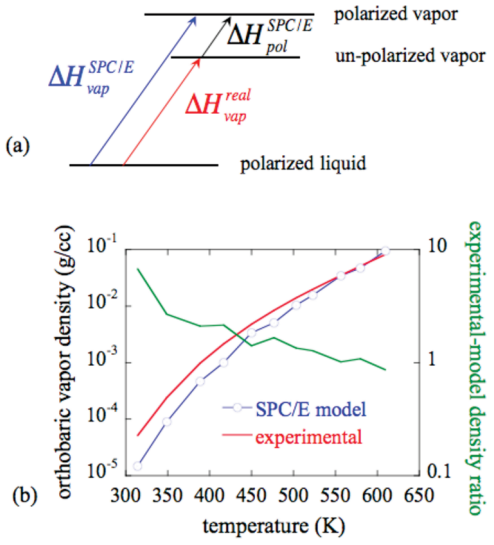

Figure 1. (a) Difference in the enthalpy of vaporization for polarized and unpolarized water molecules. (b) Vapor densities of the SPC/E model and real water. The green line shows the ratio between the experimental and SPC/E vapor densities.

are consequently nonpolarizable, and their partial electrostatic charges have fixed magnitude (i.e., "fixed-charge" models) regardless of the surrounding environment. However, these charges are augmented from the corresponding values describing the isolated (gas phase) water dipole and carbon dioxide quadrupole moments, respectively.

On one hand, because the EPM2 model was optimized to reproduce the thermodynamics of near-critical carbon dioxide, including the vapor−liquid phase envelope, this model is expected to properly describe its pure component residual chemical potential. On the other hand, the SPC/E model has been reasonably successful in the description of thermodynamic, time-dependent properties and vapor−liquid phase equilibrium of water.[5,48,49]

The SPC/E model, in contrast to its predecessor the SPC model, involves an additional "polarization correction" to the heat of vaporization to account for the "missing" water self-polarization in the liquid phase, which results in an additional enhancement of the permanent dipole moment from 2.27*D* (SPC) to 2.35*D*. While this modification greatly improves various liquid properties (i.e., the original intended target), it also causes significant deviations from the experimental values of the orthobaric vapor densities and corresponding equilibrium pressure because the fixed-charge model (with its resulting augmented dipole moment) represents an unrealistic overpolarized environment (see Figure 1a). A related situation occurs when water molecules, represented by a fixed-charge model, are transferred to a nonpolar medium such as the carbon dioxide-rich water phase in fluid−fluid equilibrium with the corresponding water-rich carbon dioxide phase.[50] Obviously, water in either a pure vapor phase or as a highly dilute solute in a nonpolar dense solvating environment exhibits comparatively smaller polarization, and consequently, a fixed-charge water model whose parameters were adjusted to describe liquid-like aqueous environments must be "depolarized" in order to properly describe real water in a nonpolar environment. A clear illustration of the consequences behind the "overpolarized" (fixed-charge) water

dx.doi.org/10.1021/jp203241q |*J. Phys. Chem. B* 2011, 115, 8775–8784

molecule is depicted in the behavior of the vapor−liquid phase envelope predicted by the SPC/E water model in Figure 1b, where the low density of water vapor at our conditions of interest exhibits relatively large deviations from the experimental values.

The overpolarization has a significant impact on the predicted water solubility in less polar environments such as those involving single phases of either carbon dioxide in a water-rich phase or water in a carbon dioxide-rich phase, and two (vapor−liquid or liquid−liquid) phases in equilibrium. For the one-phase dilute systems, the adjustment of the unlike-pair interactions can be achieved through the use of the deviation parameters (η, ξ) to match the simulated and experimental solute solubility in the desired phase.[51] However, if our target is the second scenario involving two-phases in equilibrium, we need to perform the simultaneous adjustment of the unlike-pair interactions in both phases. As we will show below (Section 2 and Appendix), this is a more challenging issue that requires a novel approach to deal with the equilibrium of phases with disparate polarities.

In the present work we propose a method for the calibration of the water−carbon dioxide unlike-pair interactions to be able to accurately describe the species solubilities in fluid−fluid phase equilibria at state conditions relevant to the geological sequestration of carbon dioxide.[50] For that purpose, in section 2 we describe a coupling parameter approach for the adjustment of the unlike-pair interactions while accounting simultaneously for the disparity of the polarization environments between the two phases in equilibrium. Because the molecular-based expressions underlying the proposed method required lengthy derivations, we included the necessary theoretical background and development of the approach in the Appendix. In section 3 we describe the application of the proposed methodology and discuss relevant thermodynamic, microstructural, and dynamics quantities obtained by molecular-based simulation. Finally, in section 4 we conclude with a summary of the main findings and future outlook.

2. THEORETICAL BACKGROUND

2.1. Coupling Parameter Approach to the Optimization of LJ Unlike-Pair Interaction Parameters. The premise behind the optimization of a molecular model for a mixture that can reproduce the experimental mutual solubility of its components is based on the (perturbative) adjustment of an existing force field (i.e., reference), which, in principle, can be done for both electrostatic and nonelectrostatic interactions. Because our goal here is to leave the pure fluid models unchanged (i.e., they are already accurate), we need only to scale the unlike-pair nonelectrostatic interaction parameters by a perturbation parameter $0 \le \theta \le \Theta$. However, even if we do not scale the electrostatic interactions of the SPC/E and EPM2 models, such a perturbation needs to be considered in the interpretation of simulation results, as we will discuss in the following subsection.

The conditions of phase equilibrium for species I between phases A and B, as described by the original (or reference $\theta = 0$) and the perturbed ($\theta = \Theta$) force fields may be written as

$$\begin{aligned} \mu_I^A(0) &= \mu_I^B(0) \\ \mu_I^A(\Theta) &= \mu_I^B(\Theta) \end{aligned} \tag{3}$$

where $\mu_I^A(0 \le \theta \le \Theta)$ denotes the chemical potential of species I in phase A, with the unlike-pair interactions scaled by θ. By invoking the coupling parameter approach[14,16] and following eqs A8, A12, and A13 of the Appendix, these conditions can be expressed in an explicit form that relates changes in the density/concentration of species I in both phases in terms of the perturbation of the unlike-pair interactions parameters,

$$\frac{\rho_I^A(0)}{\rho_I^A(\Theta)} \times \langle \exp[-\beta \sum(\Theta)] \rangle_A = \frac{\rho_I^B(0)}{\rho_I^B(\Theta)} \times \langle \exp[-\beta \sum(\Theta)] \rangle_B \tag{4}$$

where $\rho_I^A(\theta)$ is the density of species I in phase A with unlike-pair interactions scaled by θ, and $\langle\ \rangle_A$ denotes averages over the reference system (i.e., $\theta = 0$) in phase A. The symbol $\Sigma(\theta)$ represents the contribution of the perturbation $0 \le \theta \le \Theta$ to the configurational energy:[16]

$$\sum(\theta) = \varphi_i^{REF}(\xi + 2\eta^6 - \eta^{12} - 2) + \psi_i^{REF}(\eta^6 - \eta^{12})/6 \tag{5}$$

where, η and ξ are scaling factors for the LJ unlike-pair interactions parameters σ and ε as defined by eq 1 (noting that $\theta = 0$ is equivalent to $\eta = \xi = 1$). In eq 5 we have

$$\begin{aligned} \varphi_i^{REF} &= \sum_{j \ne i} u_{ij}(r_{ij}, \theta = 0); \\ \psi_i^{REF} &= \sum_{j \ne i} \left(\frac{r_{ij} \partial u_{ij}(r_{ij}, \theta = 0)}{\partial r_{ij}} \right)_{\theta = 0} \end{aligned} \tag{6}$$

where $u_{ij}(r_{ij})$ is the energy of a pair interaction between atoms i and j at separation r_{ij}.

In the particular case of fluids with low mutual miscibility, such as water and carbon dioxide, we can assume that the perturbation of unlike-pair interactions will leave the chemical potential of species I in the I-rich phase B nearly unchanged because of the high dilution of species J in phase B. Thus, from eq 4 the concentration/solubility response to the perturbation $0 \le \theta \le \Theta$ in terms of mole fractions for the species I in the I-poor phase A reduces to

$$\frac{x_I^A(\Theta)}{x_I^A(0)} \approx \frac{\rho_I^A(\Theta)}{\rho_I^A(0)} = \left\langle \exp\left[-\frac{\Sigma(\Theta)}{kT} \right] \right\rangle_A \tag{7}$$

Equations 5−7 provide a straightforward prescription for the optimization of the LJ unlike-pair interaction parameters between the SPC/E and EPM2 molecules.

2.2. Polarization Correction to the Solubility of SPC/E Water in Nonpolar Media. As highlighted in the Introduction, the point charges of the SPC/E model are fixed, though enhanced from the corresponding gas-phase values to account for the significant polarization in liquid water. Since these charges cannot adjust to values appropriate for water vapor or other less or nonpolar environments, the SPC/E water molecules are typically overpolarized in those less polar environments; consequently, they overestimate their residual enthalpy and chemical potential. The enthalpy of self-polarization of a molecule I bearing a permanent dipole moment $\vec{\mu}_I$ can be defined as $H_{pol} = 0.5(\vec{\mu}_I - \vec{\mu}_I^{vac})^2/\alpha_m$, where $\vec{\mu}_I^{vac}$ is the equilibrium dipole moment of the isolated molecule and α_m is the experimental molecular polarizability. In the case of real water $|\vec{\mu}_W^{vac}| = 1.85D$,[52] whereas for the SPC/E model (and liquid water) $|\vec{\mu}_{W,SPC/E}| = 2.35D$. Thus, while the self-polarization of SPC/E in the liquid phase is roughly equal to that of real water, the difference in self-polarization enthalpies between SPC/E and real water in a nonpolar environment corresponds to $\Delta H_{pol}^{SPC/E} = H_{pol}^{SPC/E} - H_{pol}^{real} = 0.5(\vec{\mu}_{W,SPC/E} - \vec{\mu}_W^{vac})^2/\alpha_m = 5.22$ kJ/mol. A schematic representation of the source for a difference between the self-polarization

enthalpies for a fixed-charge model and the corresponding impact on the predicted orthobaric vapor density is illustrated in Figure 1a,b.

To estimate the contribution of the molecular overpolarization on the predicted water concentration in the CO_2-rich phase, we use the coupling parameter approach developed in the Appendix. For that purpose, we take the SPC/E model as the reference system, and invoke the perturbation $0 \le \omega \le \Omega$ to rescale the atomic electrostatic charges to those corresponding to an isolated water molecule, i.e., $|\vec{\mu}_W^{vac}| = 1.85D$. For this depolarization perturbation, $\Delta H_{pol}(\Omega) = -\Delta H_{pol}^{SPC/E}$ in eq A16, i.e.,

$$\frac{x_W^C(\Omega)}{x_W^C(0)} \approx \frac{\rho_W^C(\Omega)}{\rho_W^C(0)} = \exp[+\beta \Delta H_{pol}^{SPC/E}] \times \langle \exp[-\beta \sum^{Ex}(\Omega)] \rangle_C \quad (8)$$

where phase A in this case is the one rich in carbon dioxide and denoted by the superscript "C". Note that the second term in eq 8 arises from the modified electrostatic interactions of the scaled atomic charges with the surrounding medium; consequently it would be close to unity for the case of nonpolar environments.

By combining eqs 7 and 8, we can (in principle) determine the proper scaling of the LJ unlike-pair interaction parameters, after applying the polarization correction, that will predict more accurately the solubility of water in the carbon dioxide-rich phase, i.e.,

$$\frac{x_W^C(\Theta, \Omega)}{x_W^C(0,0)} \approx \exp[+\beta \Delta H_{pol}^{SPC/E}] \times \langle \exp[-\beta \sum(\Theta)] \rangle_C \quad (9)$$

where $x_W^C(0,0)$ is the solubility (mole fraction) of water in the CO_2-rich phase predicted by the original mixture of the SPC/E and EPM2 models with the LB combining rules, and $x_W^C(\Theta,\Omega)$ is the desired water solubility. An alternative derivation of the polarization correction to the SPC/E solubility in terms of the species solvation free energies is given in the Supporting Information.

2.3. Simulation Methods. The equilibria between water-rich and carbon dioxide-rich phases were simulated by the isothermal−isobaric Gibbs ensemble Monte Carlo (NPT-GEMC) method using the Towhee software package.[53] All simulations involved systems containing a total $N = 1024$ molecules, i.e., 512 CO_2 and 512 H_2O molecules, for temperatures and pressures ranging from 298 to 348 K, and from 100 to 400 bar, respectively. The mutual CO_2/H_2O solubility at each thermodynamic state point (T, P) was calculated from the average of 3×10^5 configurations collected over $N \times 3 \times 10^6$ Monte Carlo steps. The acceptance rate of GEMC interbox transfers was approximately 4×10^{-4} for water and 2×10^{-3} for carbon dioxide molecules. The LJ interactions were truncated at 10 Å, and corrected by the long-range virial and configurational energy contributions,[54] while the long-range electrostatic interactions were treated using the Ewald summation.

For the required dynamic and microstructural properties, the corresponding isothermal−isobaric molecular dynamics simulations used LAMMPS software[55] with an added functionality for the efficient calculation of the simulation averages of the exponential term in eq 7. These systems contained a total of $N = 512$ molecules, LJ interactions were truncated at 12 Å, and the PPPM correction was used for long-range electrostatic interactions. The equations of motion were integrated using the velocity Verlet algorithm with a time step of 1 fs to cover a total length of 10 ns for each run after equilibration.

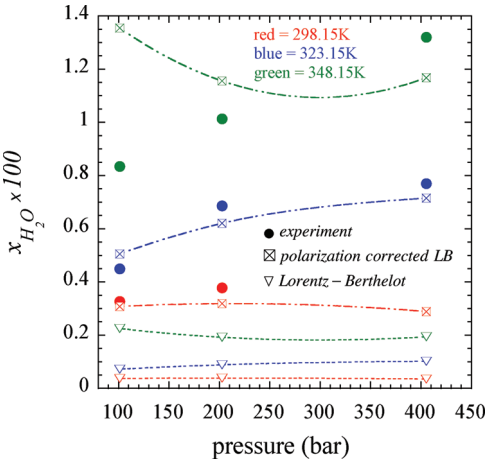

Figure 2. The effect of the polarization correction on the predicted solubility of water in supercritical CO_2 along the isotherms $T = 298.15$ K (red), $T = 323.15$ K (blue), and $T = 348.15$ K (green). Experimental data taken from refs 50, 58, 59.

3. SIMULATION RESULTS AND DISCUSSION

3.1. Mutual Solubility of Carbon Dioxide and Water. *3.1.1. Effect of the SPC/E Polarization Correction on the Water Solubility in CO_2.* As demonstrated in Section 2.2 and illustrated in Figure 1, the SPC/E model underestimates water vapor density as a consequence of the overpolarization originating from the inclusion of the self-polarization during the fixed-charge parametrization. An improved prediction of the water solubility in nonpolar environments can be obtained by scaling the values predicted from simulations by the self-polarization factor in eq 8. In fact, Figure 2 shows the effect of this scaling on the GEMC predictions of SPC/E solubility in EPM2 by the polarization correction in comparison with the corresponding experimental values. It is seen that the original predicted mole fractions (solubilities) are about an order of magnitude lower than the experimental ones. The application of the polarization correction brings the simulated solubilities within approximately 10% of the experiment at 298 and 323 K, and while the predictions for 348 K are not as accurate as those at lower temperatures, the improvement is still substantial. The larger discrepancy for the CO_2-rich phase at 348 K and 100 bar, i.e., the least polar environment, is likely to be the result of the unscreened attractive SPC/E−SPC/E dipole interactions, which contribute to the second factor on the right-hand side of eq 8. Since the dipole moment of the EPM2 model is zero, the corresponding polarization correction is also zero.

The interpretation of the SPC/E self-polarization effect on the water solubility in CO_2 should not ignore the electrostatic interactions of water with the surrounding EPM2 molecules. In the first approximation, this contribution can be neglected because carbon dioxide is nonpolar, but its electrostatic charges will interact with those of water, leading to a nonzero contribution to the second term on the right-hand side of eq 8. We can expect that the larger SPC/E dipole moment $\vec{\mu}_{W,SPC/E}$ compared to real water will result in increased attractive interactions and solubility in EPM2. Since we do not rescale the SPC/E atomic charges, we cannot correct directly for the stronger electrostatic interactions. However, assuming that the effect is small, we can try to compensate it by

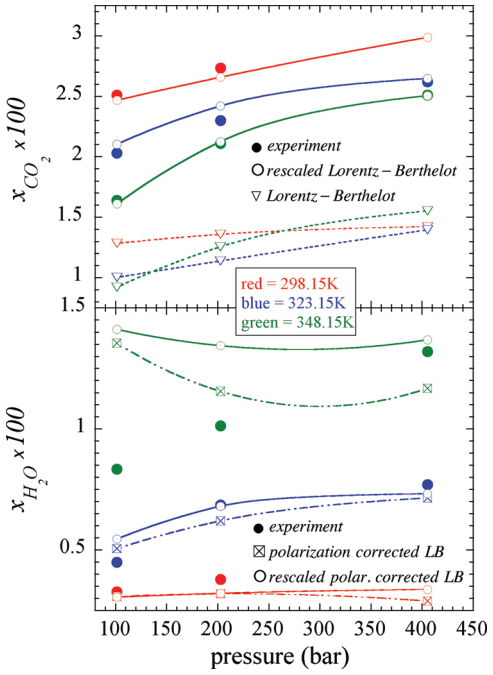

Figure 3. Solubility (molar fraction) of CO_2 in H_2O and H_2O in CO_2. Comparison between the simulation results for the polarization corrected LB system, the corresponding rescaled cross-interactions, and the available experimental data, along the same three isotherm as in Figure 2.

scaling the LJ unlike-pair interactions, as described in the following subsection.

To estimate the effect of rescaling the SPC/E charges on solubility in CO_2 and to validate the assumptions from the previous paragraph, we used eq A15 to calculate the second factor in eq 8. We found that if the SPC/E point charges are scaled down to the values corresponding to the water dipole moment in vacuum, $|\vec{\mu}_W^{vac}| = 1.85D$, the solubility is predicted to decrease by the factor of 0.73 (at $T = 348$ K and $P = 100$ bar) to 0.23 (at $T = 298$ K and $P = 400$ bar). Such changes in solubility are less significant than those coming from the self-polarization correction and are comparable to the LJ corrections discussed below.

In general, the polarization correction is added at the end of a run to interpret simulation results. It may be possible to incorporate this correction within the GEMC procedure to weigh interbox transfers, but such a direct application cannot be used in other MC or MD calculations containing explicit phase interfaces. It is also important to consider the polarization effect and the corresponding correction even in simulations of a single nonpolar phase in which SPC/E water is dissolved. If the lower solubility of the SPC/E is not considered, using experimental water concentration for simulations of a bulk carbon dioxide-rich phase in contact with mineral interfaces may result in unphysical phase separation and the formation of a water rich phase. In such cases, appropriate SPC/E concentrations can be estimated from experimental values and the polarization correction. However, given the large (10x) effect of polarization on the solubility of water in carbon dioxide, the use of polarizable models should be preferred, when possible.

3.1.2. Scaling of the LJ Unlike-Pair Interactions. The polarization correction, as applied to the SPC/E model, brings the solubility in EPM2 to experimental values but only solves the discrepancies caused by the imperfect description of the pure component. As Figure 3 shows, the solubility of EPM2 carbon dioxide in SPC/E water is considerably underestimated and needs to be increased by about 60% to be in better agreement with the experimental values. The challenge in the optimization of unlike-pair interactions is therefore to increase the average attractive interactions in one phase while leaving the interactions almost unchanged in the other phase. Given the high computational demand of the GEMC simulations, this could be a difficult and time-consuming task for a trial-and-error approach. The proposed alternative, i.e. the coupling parameter approach, allows us to try out millions of combinations of the four LJ unlike-pair interaction parameters (eq 1) and choose the best one via the global search minimization of the mean square deviations between the left- and right-hand sides of eq 7 (or eq 9 for the SPC/E).

In the first step, we chose the LB system as a reference and carried out GEMC simulations to calculate the reference solubility (mole fractions) $x_I^A(0)$, of both species in both phases as well as the configurational average quantities in eq 6. Using experimental solubility data for the desired species (mole fraction) $x_I^A(\Theta)$, we found the optimal LJ unlike-pair interaction parameters (actually, the optimal $\eta-\xi$ pair) in eq 5, as given in Table 2. Since some of the parameters were scaled by as much as 20%, the perturbation basis of the coupling parameter method might limit the precision of the results. With the exception of H_2O in CO_2 at 348 K, the predicted mutual solubilities in both phases obtained with the new set of

Table 2. LJ Cross-Parameters for the SPC/E and EPM2 Interactions Derived from the LB Rules, after the First Iteration (1st Iter.) and Second/Final Iteration (2nd Iter.) of the Scaling According to eq 8

atom type	σ_{ij} [Å]	ε_{ij} [kJ/mol]
C_C-O_W (LB)	2.9615	0.3899
O_C-O_W (LB)	3.0995	0.6597
C_C-O_W (1st iter.)	2.8815	0.4796
O_C-O_W (1st iter.)	3.1367	0.7587
C_C-O_W (2^{nd} iter.)	**2.8412**	**0.5511**
O_C-O_W (2^{nd} iter.)	**3.1524**	**0.7488**

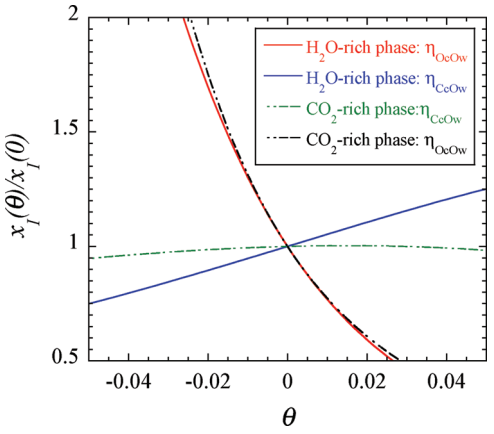

Figure 4. Dependence of the predicted solubility (left-hand side of eq 7) on the coupling parameter, $\theta = \eta - 1$, i.e., through the scaling the σ parameter of LJ potential for a system at $T = 298$ K and $P = 100$ bar.

dx.doi.org/10.1021/jp203241q |*J. Phys. Chem. B* 2011, 115, 8775–8784

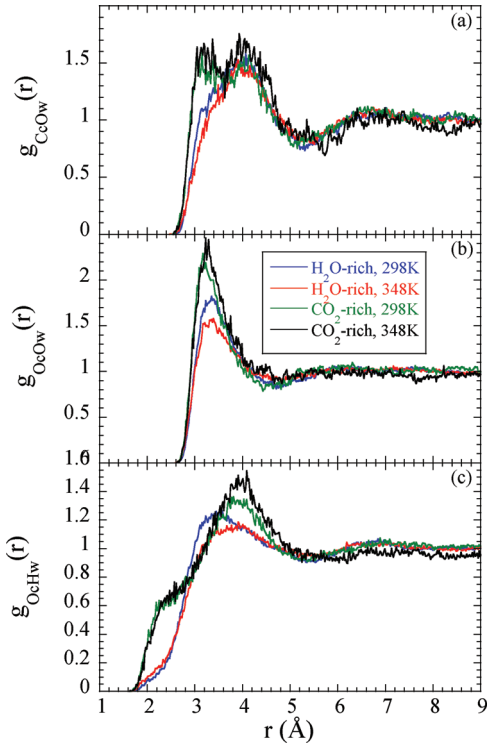

Figure 5. Comparison of the relevant pair distribution functions between the H_2O-rich and the CO_2-rich phases at 298 K and 400 bar as well as at 348 K and 100 bar.

parameters were within 10% of the experimental values (these intermediate results are not shown). We performed an additional iteration using the new parameters to define a new reference system for further refinement of the predictions. To illustrate the procedure, Figure 4 displays the dependence of the mutual solubility on the coupling parameter $\theta = \eta - 1$ as predicted by eq 7. It is interesting to notice that scaling of the LJ size parameters of the $C_C - O_W$ and $O_C - O_W$ interactions has the opposite effect on solubilities. While decreasing σ_{OcOw} leads to a considerable increase in mutual solubility in both phases, decreasing σ_{CcOw} leads to a decrease in mutual solubility, especially in the H_2O-rich phase. The origin of such relations can be traced back to differences in the solvation structures as discussed in the following subsection.

The final set of LJ unlike-pair interactions parameters is listed in Table 2 while the predicted solubilities are displayed in Figure 3. With the exception of the CO_2-rich phase at 348 K, the agreement between simulation and experiment is within 10% for all systems, which roughly corresponds to the simulation error.

3.2. Structural Properties. As has been noted earlier, the different response of the mutual solubilities (in the two phases in fluid−fluid equilibrium) to the same perturbation in force field parameters is a result of different structural arrangements of the interacting molecules. To gain better insight into the origin of these dependencies and limitations of the simple point charge models, we analyze in Figure 5 the relevant CO_2-H_2O atom−atom pair distribution functions obtained at two sets of thermodynamic conditions (higher density at $T = 298$ K and $P = 400$ bar, and lower density at $T = 348$ K and $P = 100$ bar).

These results indicate that the atomic sites involving different molecules are closer in the CO_2-rich phase than in the corresponding H_2O-rich phase. The primary reason is the formation of stronger hydrogen bonds between an isolated water molecule interacting with the surrounding oxygens from the carbon dioxide environment, whose signature can be recognized as a shoulder on the O_C-H_W (CO_2 oxygen/H_2O hydrogen) pair distribution function around 2.2 Å. If a hydrogen bond is geometrically defined as an O−H pair at separations less than 2.5 Å,[56] then a dissolved water molecule in the CO_2 surroundings would form 1.1 bonds (at 298 K and 400 bar). In contrast, in the water-rich phase the hydrogen bonding capacity of a water molecule can be saturated by other water molecules, resulting in less opportunity for CO_2 oxygens to participate in such interactions. On average, a dissolved CO_2 molecule forms 0.7 hydrogen bonds.

Table 3. Simulated (sim.) and Experimental (exp.) Diffusion Coefficients of Infinite Diluted CO_2 in Water, D_{CO2}, and H_2O in Carbon Dioxide, D_{H2O}

T [K]/ P [bar]	D_{CO2} [10^{-5} cm^2/s] sim./exp.	T [K]/ P [bar]	D_{H2O} [10^{-4} cm^2/s] sim./exp.
298/1.0325	1.98/1.95[a]	298/202.65	1.54/1.59[b]
323/1.0325	3.57/3.03[a]	323/202.65	1.96
348/1.0325	5.74/5.40[a]	348/202.65	2.70
298/101.325	2.00	298/101.325	2.65
298/202.65	2.10	298/202.65	1.86
298/405.3	1.98	298/405.3	1.71

[a] Reference 60. [b] Reference 61.

The shape of the C_C-O_W pair distribution function in Figure 5 also elucidates the reason for the solubility reduction with decreasing σ_{CcOw}: the majority of the C_C-O_W atom pairs are located beyond the minimum of the LJ potential (i.e., $r > 2^{1/6}\sigma_{CO_w} \approx 3.19$ Å) of this interaction, so that a shift of the minimum to shorter separations leads to an increase in the pair energy. The opposite trend is seen for the O_C-O_W pairs where most of the nearest neighbors are separated by less than the LJ minimum ($r > 2^{1/6}\sigma_{O_cO_w} \approx 3.54$ Å).

3.3. Dynamic Properties. An additional typical requirement for the adequacy of molecular models is the accurate description of dynamic properties. To assess the performance of our proposed optimized unlike-pair interactions, we determined by isothermal−isobaric molecular dynamics simulations the (tracer) diffusion coefficients D_I for infinitely diluted species I in species J using the Einstein formula,

$$D_I = \lim_{t \to \infty} \frac{\langle (r_i(t) - r_i(0))^2 \rangle}{6t} \qquad (10)$$

where $r_i(t)$ is the unfolded position of the solute particle i at time t, and $\langle\ \rangle$ indicate an average over simulation trajectories (time origin of a single long trajectory). The simulated diffusion coefficients of water in carbon dioxide and carbon dioxide in water are listed in Table 3, and compared with available experimental data in Figure 6. The simulated carbon dioxide diffusion in water is in a fairly good agreement with experimental values in the whole range of investigated temperatures, which is a significant improvement over the predictions of these mixtures under LB combining rules for which the simulation overpredicts the CO_2 diffusivity by 30%. The diffusion coefficient of water in CO_2, D_{H2O}, at 298 K is about 20% higher than

dx.doi.org/10.1021/jp203241q |J. Phys. Chem. B 2011, 115, 8775–8784

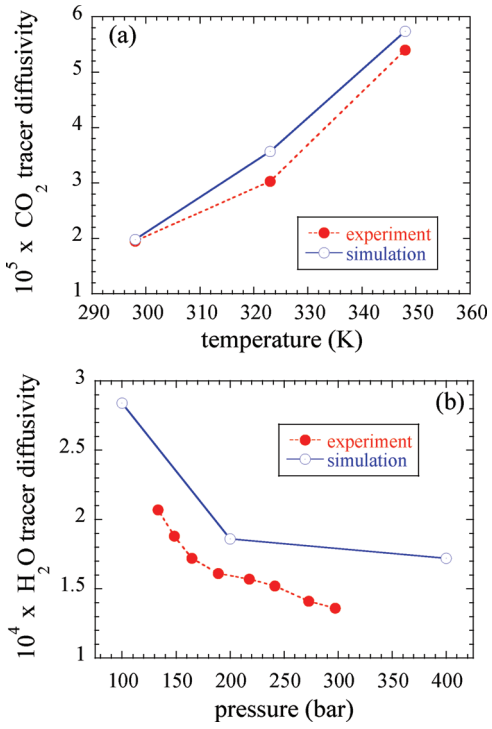

Figure 6. (a) Temperature dependence of the diffusion coefficient of infinitely diluted CO_2 in liquid water at 1 bar, D_{CO2}; (b) pressure dependence of the diffusion coefficient of infinitely diluted H_2O in carbon dioxide at 298 K. Experimental data and simulation results are in the units of cm^2s^{-1}.

the experimental values and closer than those predicted by the LB system, while it shows the correct pressure dependence. It is possible that the higher diffusivity of D_{H2O} at 298 K is governed by the same factors that cause the lower solubility of H_2O in CO_2 at the same temperature, but we did not find experimental data for higher temperatures to verify this relation and our conjecture.

4. CONCLUDING REMARKS

We proposed and applied a coupling parameter scheme to optimize the SPC/E-EPM2 pair interactions to reproduce the mutual solubility of carbon dioxide and water at conditions typical for carbon dioxide sequestration. We found that when the self-polarization correction for the chemical potential of SPC/E water in the CO_2-rich phase is included, the predicted solubilities are generally within the simulation/experimental combined uncertainties. The adequacy and reliability of the scaled LJ unlike-pair interactions were then supported by the reasonable predictions of the diffusion coefficients of the dilute species in both phases. Considering that our method included global optimization in the force field parameter space, we expect that the current parameter set is close to optimal and could not be significantly improved without changing the pure-component models, e.g., by adding explicit polarizability or chemical reactivity. The use of the original SPC/E and EPM2 parametrization for the same component interactions allows us to build on the large database of published force fields and simulation data obtained for pure CO_2 and H_2O in contact with diverse environments.

APPENDIX: PERTURBATION OF THE SPECIES CHEMICAL POTENTIAL IN THE GIBBS ISOTHERMAL−ISOBARIC ENSEMBLE

Here we derive the equations for the isothermal−isobaric change of the chemical potential of a species in two equilibrated phases due to the perturbations of the force field parameters of a molecular model. We are not only interested in the effect of the perturbation $0 \le \theta \le \Theta$ of the LJ unlike-pair interaction parameters, but also in that of the perturbation $0 \le \omega \le \Omega$ of the electrostatic interactions on the species chemical potential. For that purpose we express the chemical potential of species I in terms of the coupling parameters Θ and Ω as follows:

$$\mu_I(T,P,x_I,\Theta,\Omega) = (\partial G/\partial N_I)_{T,P,N_{J\neq I}}$$
$$\simeq [G(N_I+1,\theta=\Theta,\omega=\Omega) - G(N_I,\theta=0,\omega=0)]_{T,P,N_{J\neq I}}$$
$$= -kT\ln\left[\frac{Q_{GE}(N_I+1,\theta=\Theta,\omega=\Omega)}{Q_{GE}(N_I,\theta=0,\omega=0)}\right]_{T,P,N_{J\neq I}} \quad (A1)$$

where $[G(N_I,\theta,\omega)]_{T,P,N_{J\neq I}}$ is the total Gibbs free energy of the system of $N = N_I + \Sigma_{J\neq I}N_J$ particles of types I and J, at constant pressure P, temperature T, and number of particles of type J. The molar fraction of species I is defined as $x_I = N_I/N$, and $[Q_{GE}(N_I,\theta,\omega)]_{T,P,N_{J\neq I}}$ is the corresponding isothermal−isobaric Gibbs ensemble (GE) partition function.

Typically, the description of equilibria between phases A and B via the GE simulation approach involves two separate boxes, which we identify here by the phases they are containing (either A or B). Moreover, because we will deal with the chemical potential of a specific species in a mixture, we drop the subscript I in the following analysis and, for simplicity, derive the statistical mechanical relations as if we were dealing with a single-component system. Subsequently, the multicomponent expressions are straightforwardly obtained and left to the reader. The GE partition function for the above system can be written as[57]

$$Q_{GE}(N,T,P,\theta,\omega)$$
$$= \Lambda^{-3N}\sum_{n=0}^{N}\Delta_A(n,T,P,\theta,\omega)\Delta_B(N-n,T,P,\theta,\omega) \quad (A2)$$

where Λ is the de Broglie wavelength, $\beta = 1/kT$, k is the Boltzmann constant, n is the number of particles in box A, and $\Delta_\alpha(n,P,T,\theta,\omega)$ is the isobaric−isothermal configurational partition function for the corresponding box α. Moreover,

$$\Delta_\alpha(n,P,T,\theta,\omega)$$
$$= \frac{1}{n!}\int_0^\infty \exp(-\beta PV_\alpha)\,dV_\alpha \int_{V_\alpha}\exp(-\beta U_\alpha(r^n,\theta,\omega))\,dr^n \quad (A3)$$

where $U_\alpha(r^n,\theta,\omega)$ is the total potential energy in box α for the specific configuration defined by r^n, and current strength of the coupling parameters θ and ω. The coupling parameters enable to determine the working equation for the chemical potential of species I in either phase, and its change caused by any perturbation of the unlike-pair interactions. Consequently, the potential energy of the $(n+1)$-system can be described as $U_\alpha(r^{n+1},\lambda,\theta,\omega) = U_\alpha(r^n) + \lambda u_\alpha + \Sigma(\theta) + \Sigma(\omega)$, where we invoked an additional coupling parameter λ, which turns on (1) and off (0) the interactions u_α of the $(n+1)$th particle with the rest of box α, and the two $\Sigma(\cdots)$ terms represent contributions to a particle energy due to the perturbations of the two coupling parameters θ and ω. For the full interaction of the $(n+1)$th particle of the unperturbed system

dx.doi.org/10.1021/jp203241q | J. Phys. Chem. B 2011, 115, 8775–8784

(i.e., $\lambda = 1$), the notations $Q_{GE}(N+1,\lambda=1)$ and $Q_{GE}(N+1)$ are equivalent. According to the description for $U_\alpha(r^{n+1},\lambda,\theta,\omega)$, eq A1 can be decomposed into four terms as follows:

$$\mu(T,P,\Theta,\Omega) = -kT\ln\left[\underbrace{\frac{Q_{GE}(N+1,\lambda=0)}{Q_{GE}(N)}}_{\langle V\rangle_{GE,T,P,N}/[(N+1)\Lambda^3]}\times\underbrace{\frac{Q_{GE}(N+1,\lambda=1)}{Q_{GE}(N+1,\lambda=0)}}_{\exp[-\beta\mu^{conf}]}\times\right.$$
$$\left.\underbrace{\frac{Q_{GE}(N+1,\theta=\Theta)}{Q_{GE}(N+1,\theta=0)}}_{\exp[-\beta\Delta\mu^{vdW}]}\times\underbrace{\frac{Q_{GE}(N+1,\omega=\Omega)}{Q_{GE}(N+1,\omega=0)}}_{\exp[-\beta\Delta\mu^{Coul}]}\right]_{T,i} \quad \text{(A4)}$$

where $\rho = \langle V\rangle/(N+1)$ is the average number density of species I, the first factor in the logarithm corresponds to the contribution of the ideal gas at density ρ, the second corresponds to the configurational contribution of the reference system, the third is the contribution from the perturbation θ of the van der Waals (nonelectrostatic) interactions, and the fourth is the contribution due to the perturbation ω of electrostatic interactions (site partial charges). Note that eq A4 is written for the ensemble of two boxes as a whole because the chemical potential of a particle in the GE cannot be expressed solely in terms of a single phase.[57]

Phase Equilibrium of the Reference System. For the explicit analysis of phase equilibria via the GE, we define a pair of coupling parameters λ_A and λ_B, which turn on the interactions of a single particle of type I in each box (A or B) separately. The first two factors in eq A4 (unperturbed system) can then be written as

$$\frac{Q_{GE}(N+1,\lambda=0)}{Q_{GE}(N)}\times\frac{Q_{GE}(N+1,\lambda=1)}{Q_{GE}(N+1,\lambda=0)}$$
$$=\begin{cases}\dfrac{Q_{GE}(N+1,\lambda_A=0,\lambda_B=1)}{Q_{GE}(N)}\times\dfrac{Q_{GE}(N+1,\lambda_A=1,\lambda_B=1)}{Q_{GE}(N+1,\lambda_A=0,\lambda_B=1)}\\ \dfrac{Q_{GE}(N+1,\lambda_A=1,\lambda_B=0)}{Q_{GE}(N)}\times\dfrac{Q_{GE}(N+1,\lambda_A=1,\lambda_B=1)}{Q_{GE}(N+1,\lambda_A=1,\lambda_B=0)}\end{cases} \quad \text{(A5)}$$

where

$$\frac{Q_{GE}(N+1,\lambda_A=0,\lambda_B=1)}{Q_{GE}(N)} = \frac{\sum_{n=0}^{N+1}\Delta_A(n,T,P,\lambda_A=0)\Delta_B(N+1-n,T,P)}{\Lambda^3\times\sum_{n=0}^{N}\Delta_A(n,T,P)\Delta_B(N-n,T,P)}$$
$$=\frac{\sum_{n=0}^{N}[\Delta_A(n+1,T,P,\lambda_A=0)\Delta_B(N-n,T,P)]+\Delta_B(N+1,T,P)}{\Lambda^3\times\sum_{n=0}^{N}\Delta_A(n,T,P)\Delta_B(N-n,T,P)}$$
$$\frac{Q_{GE}(N+1,\lambda_A=1,\lambda_B=1)}{Q_{GE}(N+1,\lambda_A=0,\lambda_B=1)} = \frac{\sum_{n=0}^{N+1}\Delta_A(n,T,P,\lambda_A=1)\Delta_B(N+1-n,T,P,\lambda_B=1)}{\sum_{n=0}^{N+1}\Delta_A(n,T,P,\lambda_A=0)\Delta_B(N+1-n,T,P,\lambda_B=1)} \quad \text{(A6)}$$

Following the Smit and Frenkel approach,[57] these equations can be rewritten in the form of ensemble averages and interpreted as the equality of activities between two phases in equilibrium, i.e.,

$$\Lambda^{-3}\left\langle\frac{V_A}{n+1}+\delta_{n,0}\frac{V_B}{N-n+1}\exp(-\beta u_B)\right\rangle\times\langle\exp(-\beta u_A)\rangle_{\lambda_A=0} =$$
$$=\Lambda^{-3}\left\langle\frac{V_B}{N+1-n}+\delta_{n,N}\frac{V_A}{n+1}\exp(-\beta u_A)\right\rangle\times\langle\exp(-\beta u_B)\rangle_{\lambda_B=0} \quad \text{(A7)}$$

Because the terms involving the Kronecker delta $\delta_{n,X}$ can be neglected for a large enough total number of particles N, we can recover the familiar expression for the equilibrium conditions in terms of equality of the activities/chemical potentials,

$$\frac{1}{\langle\Lambda^3\rho^A\rangle}\times\langle\exp(-\beta u_A)\rangle_{\lambda_A=0} = \frac{1}{\langle\Lambda^3\rho^B\rangle}\times\langle\exp(-\beta u_B)\rangle_{\lambda_b=0}$$
$$kT\ln\langle\Lambda^3\rho^A\rangle - kT\ln\langle\exp(-\beta u_A)\rangle_{\lambda_A=0}$$
$$= kT\ln\langle\Lambda^3\rho^B\rangle - kT\ln\langle\exp(-\beta u_B)\rangle_{\lambda_B=0} \quad \text{(A8)}$$

where ρ^α is the number density of species I in box α. The two terms on each side of the second line of eq A8 correspond to the chemical potential of the ideal gas (at the average density $\langle\rho_\alpha\rangle$ and temperature T), and to the configurational contribution of species I, respectively. Similar equations can be derived for the chemical potential of species I in a mixture if the potential energy u_α includes interactions with other species. In the following text, a mixture of species I and J is explicitly considered.

Perturbation of the LJ Unlike-Pair Interactions. The third factor in eq A4 involves a contribution to the configurational chemical potential of species I due to the perturbation of nonelectrostatic unlike-pair interaction parameters. In general, this perturbation will affect the particle interactions in both phases, which will result in a modified density/composition of each phase. Recalling that one of the main goals of this paper is to find a relation between the perturbation of the unlike-pair interaction parameters and the changes of the species mutual solubility, we express the change of the species residual chemical potential in each phase as a function of the perturbed LJ unlike-pair interaction parameters and calculate the corresponding change in the species composition from the condition of phase equilibria (eq A8).

The change in the configurational portion of the chemical potential of species I, for a large N, can be expressed for each phase separately as

$$\Delta\mu_I^{conf,A}(T,P,x_I) = -kT\ln\left[\frac{Q_{GE}(N_I+1,\theta=\Theta)}{Q_{GE}(N_I+1,\theta=0)}\right]_{T,P,N_{J\neq I}}$$
$$= -kT\ln\frac{\sum_{n_I=0}^{N+1}\Delta_A(n_I,P,T,\theta=\Theta)\Delta_B(N+1-n_I,P,T,\theta=0)}{\sum_{n_I=0}^{N+1}\Delta_A(n_I,P,T,\theta=0)\Delta_B(N+1-n_I,P,T,\theta=0)}$$
$$= -kT\ln\langle\exp[-\beta\Sigma(\theta=\Theta)]\rangle_A \quad \text{(A9)}$$

where n_I is the number of particles of species I in box A, $\langle\ \rangle_A$ denotes the GE average over the reference system in box A, and $\Sigma(\Theta) = U_{N+1}(N_I+1,N_J,\theta=\Theta) - U_{N+1}(N_I+1,N_J,\theta=0)$ is the difference in potential energy of a particle i of species I caused by

the perturbation $0 \le \theta \le \Theta$, which can be defined in terms of the deviations η and ξ from the corresponding reference system (e.g., see eq 2) comprising the combining rules for the LJ unlike-pair interaction parameters σ_{ij} and ε_{ij}, respectively, i.e.,

$$\sum(\theta) = \varphi_i^{\mathrm{REF}}(\xi + 2\eta^6 - \eta^{12} - 2) + \psi_i^{\mathrm{REF}}(\eta^6 - \eta^{12})/6 \tag{A10}$$

where $\theta = 0$ is equivalent to $\eta = \xi = 1$, and

$$\varphi_i^{\mathrm{REF}} = \sum_{j \neq i} u_{ij}(r_{ij}, \theta = 0);$$

$$\psi_i^{\mathrm{REF}} = \sum_{j \neq i} \left(r_{ij} \frac{\partial u_{ij}(r_{ij}, \theta = 0)}{\partial r_{ij}} \right)_{\theta = 0} \tag{A11}$$

The quantities φ_i^{REF} and ψ_i^{REF} can be calculated from the simulations of the reference system, e.g., when the unlike-pair interactions are defined by the LB combining rules.

From eq A9, the condition of phase equilibrium expressed in eq A8 for the unperturbed reference system ($\theta = 0$) can be written for the perturbed system ($\theta = \Theta$) as follows:

$$\frac{1}{\langle \Lambda^3 \rho_{\mathrm{A}}(\Theta) \rangle} \times \langle \exp(-\beta u_{\mathrm{A}}) \rangle_{\lambda_{\mathrm{A}} = 0} \times \langle \exp(\sum(\Theta)) \rangle_{\mathrm{A}}$$
$$= \frac{1}{\langle \Lambda^3 \rho_{\mathrm{B}}(\Theta) \rangle} \times \langle \exp(-\beta u_{\mathrm{B}}) \rangle_{\lambda_{\mathrm{B}} = 0} \times \langle \exp(\sum(\Theta)) \rangle_{\mathrm{B}} \tag{A12}$$

Consequently, from eqs A9 and A12 we obtain the relation for the corresponding change in species densities (concentrations) in both phases as a function of perturbation parameter $0 \le \theta \le \Theta$, i.e.,

$$\frac{\rho_{\mathrm{I}}^{\mathrm{A}}(0)}{\rho_{\mathrm{I}}^{\mathrm{A}}(\Theta)} \times \langle \exp[-\beta \sum(\Theta)] \rangle_{\mathrm{A}}$$
$$= \frac{\rho_{\mathrm{I}}^{\mathrm{B}}(0)}{\rho_{\mathrm{I}}^{\mathrm{B}}(\Theta)} \times \langle \exp[-\beta \sum(\Theta)] \rangle_{\mathrm{B}} \tag{A13}$$

The significance of this equation is that it can be used to optimize force field parameters so that the model system reproduces experimental mutual solubilities of species between two phases in equilibrium. A simplified relation can be found for a mixture of two species I and J with low mutual solubility, such as water and carbon dioxide, in which one of the two phases is typically nearly pure species I and the other comprises nearly pure species J. Due to the low concentration of species J in the I-rich phase B, the residual part of the activity of species I in phase B is unaffected by the changes in the unlike-pair interactions. Moreover, due to the high concentration of species I in phase B, the ratio of densities $\rho_I^{\mathrm{B}}(0)/\rho_I^{\mathrm{B}}(\Theta)$ is barely changed even for relatively large changes in the ratio $\rho_I^{\mathrm{A}}(0)/\rho_I^{\mathrm{A}}(\Theta)$. These two statements express the fact that the change in activity/chemical potential of species I in the I-rich phase is negligible, which allows us to establish the following approximate relation between the perturbation of the LJ unlike-pair interaction parameters and the change of the species I concentration in the I-poor (J-rich) phase.

$$\frac{\rho_I^{\mathrm{A}}(\Theta)}{\rho_I^{\mathrm{A}}(0)} \approx \langle \exp[-\beta \sum(\Theta)] \rangle_{\mathrm{A}} \tag{A14}$$

Perturbation of the Electrostatic Interactions. The effect of the perturbation $0 \le \omega \le \Omega$ of atomic charges on the mutual solubilities of species in each phase in equilibrium can be derived along the same approach used for eqs A9−A13. The main difference is a one-particle term corresponding to the self-polarization of a molecule, i.e., the energy required to change the charge distribution within an isolated molecule. If we assume that all atomic charges q_α in a molecule i of species I are scaled by the same factor $(1 + \Omega)$, then the energy difference in the configurational energy between the perturbed and the reference systems from the self-polarization and the interactions with atomic charges q_β of molecules j can be written as

$$\sum(\Omega) = U_{N+1}(N_{\mathrm{I}} + 1, N_j, \omega = \Omega) - U_{N+1}(N_{\mathrm{I}} + 1, N_j, \omega = 0)$$
$$= (H_{\mathrm{pol}}(\Omega) - H_{\mathrm{pol}}(0))$$
$$+ \sum_{\alpha \in i} \left[(2\Omega + \Omega^2) \times \sum_{j \in I} \sum_{i \beta \in j} \frac{q_\alpha q_\beta}{r_{\alpha\beta}} + \Omega \times \sum_{j \in J} \sum_{\beta \in j} \frac{q_\alpha q_\beta}{r_{\alpha\beta}} \right]$$
$$= \Delta H_{\mathrm{pol}} + (2\Omega + \Omega^2) \times \varphi_{iI} + \Omega \times \varphi_{iJ}$$
$$= \Delta H_{\mathrm{pol}} + \sum^{Ex}(\Omega) \tag{A15}$$

where H_{pol} is the self-polarization enthalpy, and the φ_{iI} and φ_{iJ} terms account for the sum of electrostatic pair energies of molecule i with like and unlike species, respectively.

The self-polarization term is a complicated function of electronic and nuclear interactions but can be expressed in a simplified way as a function of the experimental molecular polarizability α_m and the difference of the molecular dipole moment relative to its vacuum value $\Delta\vec{\mu}(\omega)$, as $H_{\mathrm{pol}}(\omega) = 0.5\Delta\vec{\mu}(\omega)^2/\alpha_{\mathrm{m}}$. The effect of the charge perturbation on the equilibrium species concentrations (solubilities) can be cast in the form of eq A13 with Θ replaced by Ω. Assuming a constant chemical potential of species I in phase B in equilibrium with phase A and fixed dipole moment, the relation for the change in number density/concentration for species I in phase A can be expressed as follows:

$$\frac{\rho_I^{\mathrm{A}}(\Omega)}{\rho_I^{\mathrm{A}}(0)} = \exp[-\beta \Delta H_{\mathrm{pol}}(\Omega)] \times \langle \exp[-\beta \sum^{Ex}(\Omega)] \rangle_{\mathrm{A}} \tag{A16}$$

In a non-polar environment, the second factor on the right-hand side is equal to ~1 and the change in number density/concentration is given only by the change in self-polarization. It is important to note that the self-polarization term in molecular models with fixed charges does not affect the actual simulations (i.e., it does not contribute to the equations of motion), yet, it needs to be considered in the interpretation of the simulation results and their comparison with real systems or polarizable force fields.

■ ASSOCIATED CONTENT

Supporting Information. Alternative derivation of the polarization contribution to the solubility of SPC/E water in a carbon dioxide-rich phase. This material is available free of charge via the Internet at http://pubs.acs.org.

■ AUTHOR INFORMATION

Corresponding Author

*E-mail: vlcekl1@ornl.gov. Fax: 865-574-4961.

Present Addresses

†Current address: School of Earth Sciences, Ohio State University, Columbus, OH 43210, United States.

■ ACKNOWLEDGMENT

Research sponsored by the Division of Chemical Sciences, Geosciences, and Biosciences, Office of Basic Energy Sciences, U.S. Department of Energy. Support for this work comes from the U.S. Department of Energy through the LBNL "Center for Nanoscale Control of Geologic CO_2" (FWP ERKCC67) under Contract DE-AC05-00OR22725 to Oak Ridge National Laboratory, managed and operated by UT-Battelle, LLC.

■ REFERENCES

(1) Goyal, K. P. *Geothermics* **1995**, *24*, 167.
(2) MIT Panel. The Future of Geothermal Energy; MIT: Cambridge, MA, 2006 (http://geothermal.inel.gov/publications/future_of_geothermal_energy.pdf).
(3) *Carbon Dioxide Capture and Storage: Special Report of the Intergovernmental Panel on Climate Change*; Metz, B., Davidson, O., de Coninck, H., Loos, M., Meyer, L., Eds.; Cambridge University Press: New York, 2005.
(4) Cole, D. R.; Chialvo, A. A.; Rother, G.; Vlcek, L.; Cummings, P. T. *Philos. Mag.* **2010**, *90*, 2339.
(5) Guillot, B. *J. Mol. Liq.* **2002**, *101*, 219.
(6) Murthy, C. S.; Singer, K.; McDonald, I. R. *Mol. Phys.* **1981**, *44*, 135.
(7) Moller, D.; Fischer, J. *Fluid Phase Equilib.* **1994**, *100*, 35.
(8) Potoff, J. J.; Siepmann, J. I. *AIChE J.* **2001**, *47*, 1676.
(9) Merker, T.; Engin, C.; Vrabec, J.; Hasse, H. *J. Chem. Phys.* **2010**, 132.
(10) Berendsen, H. J. C.; Grigera, J. R.; Straatsma, T. P. *J. Phys. Chem.* **1987**, *91*, 6269.
(11) Harris, J. G.; Yung, K. H. *J. Phys. Chem.* **1995**, *99*, 12021.
(12) O'Connell, J. P.; Haile, J. M. *Thermodynamics: Fundamentals for Applications*; Cambridge University Press: New York, 2005.
(13) Shukla, K. P.; Haile, J. M. *Mol. Phys.* **1988**, *64*, 1041.
(14) Fischer, J.; Möller, D.; Chialvo, A. A.; Haile, J. M. *Fluid Phase Equilib.* **1989**, *48*, 161.
(15) Chialvo, A. A. *J. Chem. Phys.* **1990**, *92*, 673.
(16) Chialvo, A. A. *Mol. Phys.* **1991**, *73*, 127.
(17) Fotouh, K.; Shukla, K. *Fluid Phase Equilib.* **1997**, *135*, 35.
(18) Kohler, F. *Monatsh. Chem.* **1957**, *88*, 857.
(19) Hudson, G. H.; McCoubrey, J. C. *Trans. Faraday Soc.* **1960**, *56*, 761.
(20) Kohler, F.; Fischer, J.; Wilhelm, E. *J. Mol. Struct.* **1982**, *84*, 245.
(21) Kohler, F.; Pfennig, A. *Pure Appl. Chem.* **1989**, *61*, 1041.
(22) Fender, B. E. F.; Halsey, G. D. *J. Chem. Phys.* **1962**, *36*, 1881.
(23) Hiza, M. J.; Duncan, A. G. *AIChE J.* **1970**, *16*, 733.
(24) Sikora, P. T. *J. Phys., Part B: At. Mol. Phys.* **1970**, *3*, 1475.
(25) Good, R. J.; Hope, C. J. *J. Chem. Phys.* **1970**, *53*, 540.
(26) Kong, C. L. *J. Chem. Phys.* **1973**, *59*, 968.
(27) Pena, M. D.; Pando, C.; Renuncio, J. A. R. *J. Chem. Phys.* **1982**, *76*, 333.
(28) Tang, K. T.; Toennies, J. P. *Chem. Phys.* **1991**, *156*, 413.
(29) Halgren, T. A. *J. Am. Chem. Soc.* **1992**, *114*, 7827.
(30) Waldman, M.; Hagler, A. T. *J. Comput. Chem.* **1993**, *14*, 1077.
(31) Singer, J. V. L.; Singer, K. *Mol. Phys.* **1972**, *24*, 357.
(32) Kirkwood, J. G. *J. Chem. Phys.* **1935**, *3*, 300.
(33) Kirkwood, J. G. *Chem. Rev.* **1936**, *19*, 275.
(34) Duh, D. M.; Henderson, D.; Rowley, R. L. *Mol. Phys.* **1997**, *91*, 1143.
(35) Rouha, M.; Moucka, F.; Nezbeda, I. *Collect. Czech. Chem. Commun.* **2008**, *73*, 533.
(36) Rouha, M.; Nezbeda, I. *Fluid Phase Equilib.* **2009**, *277*, 42.
(37) Delhommelle, J.; Millie, P. *Mol. Phys.* **2001**, *99*, 619.
(38) Schnabel, T.; Vrabec, J.; Hasse, H. *J. Mol. Liq.* **2007**, *135*, 170.
(39) Boda, D.; Henderson, D. *Mol. Phys.* **2008**, *106*, 2367.
(40) Forsman, J.; Woodward, C. E. *Langmuir* **2010**, *26*, 4555.
(41) McDonald, I. R. *Mol. Phys.* **1972**, *23*, 41.
(42) Bohn, M.; Fischer, J.; Kohler, F. *Fluid Phase Equilib.* **1986**, *31*, 233.
(43) Calado, J. C. G.; Filipe, E. J. M.; Lopes, J. N. C.; Lucio, J. M. R.; Martins, J. F.; Martins, L. F. G. *J. Phys. Chem. B* **1997**, *101*, 7135.
(44) Slusher, J. T. *Fluid Phase Equilib.* **1999**, *154*, 181.
(45) Koyuncu, M.; Demirtas, A.; Ogul, R. *Fluid Phase Equilib.* **2002**, *193*, 87.
(46) Huang, Y. L.; Vrabec, J.; Hasse, H. *Fluid Phase Equilib.* **2009**, *287*, 62.
(47) Potoff, J. J.; Errington, J. R.; Panagiotopoulos, A. Z. *Mol. Phys.* **1999**, *97*, 1073.
(48) Errington, J. R.; Panagiotopoulos, A. Z. *J. Phys. Chem. B* **1998**, *102*, 7470.
(49) Gonzalez, M. A.; Abascal, J. L. F. *J. Chem. Phys.* **2010**, *132*, 096101.
(50) Spycher, N.; Pruess, K.; Ennis-King, J. *Geochim. Cosmochim. Acta* **2003**, *67*, 3015.
(51) Chialvo, A. A.; Vlcek, L.; Cole, D. R. To be submitted to *J. Phys. Chem. C*, 2011.
(52) Eisenberg, D.; Kauzmann, W. *The Structure and Properties of Water*; Oxford University Press: New York, 1969.
(53) Martin, M. G.; Siepmann, J. I. *J. Phys. Chem. B* **1999**, *103*, 4508.
(54) Allen, M. P.; Tildesley, D. J. *Computer Simulation of Liquids*; Oxford University Press: Oxford, 1987.
(55) Zhang, Y. G.; Guo, G. J.; Refson, K.; Zhao, Y. J. *J. Phys.: Condens. Matter* **2004**, *16*, 9127.
(56) Jeffrey, G. A. *An Introduction to Hydrogen Bonding*; Oxford University Press: Oxford, 1997.
(57) Smit, B.; Frenkel, D. *Mol. Phys.* **1989**, *68*, 951.
(58) Wiebe, R.; Gaddy, V. L. *J. Am. Chem. Soc.* **1941**, *63*, 475.
(59) King, M. B.; Mubarak, A.; Kim, J. D.; Bott, T. R. *J. Supercrit. Fluids* **1992**, *5*, 296.
(60) Xu, B.; Nagashima, K.; DeSimone, J. M.; Johnson, C. S. *J. Phys. Chem. A* **2003**, *107*, 1.
(61) Espinoza, D. N.; Santamarina, J. C. *Water Resour. Res.* **2010**, *46*, W07537.